Equilibrium Reference Point Calculations for the Next Generation of Spatial Assessments

Kapur, M.S.[1], Siple, M.C.[2], Olmos, M. [3], Privitera-Johnson, K.M.[1], Adams, G. [1], Best, J. [4], Castillo-Jordán, C. [5], Cronin-Fine, L. [4], Havron, A.M. [6], Lee, Q. [1], Methot, R.D. [7], Punt, André E. [1]

[1]School of Aquatic and Fisheries Sciences, University of Washington, Seattle, WA 98195, USA
[2]Resource Assessment and Conservation Engineering Division, Alaska Fisheries Science Center, National Oceanic and Atmospheric Administration, 7600 Sand Point Way N.E., Seattle, WA 98115
[3]College of Earth, Ocean, and Atmospheric Sciences, Oregon State University, Corvallis, OR 97330, USA
[4]Quantitative Ecology and Resource Management, University of Washington, Ocean Teaching Building, Suite 300, Seattle, WA, Box 357941, 98195, USA
[5]Oceanic Fisheries Programme, The Pacific Community (SPC), B.P. D5, 98848 Nouméa, New Caledonia
[6]ECS Federal in support of National Oceanic and Atmospheric Administration Office of Science & and Technology, 1315 East-West Boulevard, Silver Spring, MD, 20910, USA
[7]National Marine Fisheries Service, Silver Spring, MD, USA

Abstract

Fish populations with spatial structure inherently violate the assumption of a single well-mixed stock, necessitating the use of spatially-structured population dynamics models. Accounting for spatial structure accurately and easily is a major goal for the next generation of stock assessment software development. Reference points (e.g., **limit or target harvest rates and their associated biomass**) are inherent to stock assessments and are often calculated under equilibrium conditions. However, the calculation process can be challenging for spatially-structured population dynamics models. We outline how to calculate equilibrium quantities within spatially-structured models where density-dependence in recruitment is local. We compare those values to equivalent situations when density-dependence in recruitment is global, thereby extending the set of population dynamics models on which spatially-structured stock assessments could be based. **Results suggest that our method for calculating reference points under the assumption of local density-dependence can be performed using a straightforward optimization routine, and provide clearer understanding of the effects of fishing on a spatially-structured population.** Finally, we address areas of research and development needed to integrate spatially-structured population dynamics models within existing management systems.

Keywords Fisheries assessment; Fisheries management; Recruitment; Spatial dynamics

1. Introduction

Fisheries scientists have long recognized the need to appropriately account for spatial heterogeneity in stock assessments (e.g., Beverton and Holt, 1957; Schaefer, 1968). The interaction of biological and environmental processes, and spatial exploitation patterns, can lead demographic rates (i.e., growth, death, immigration, and emigration) to vary across space, resulting in observable spatial patterns in fish populations and yields. Ignoring spatial structure in assessments can lead to bias in estimated management quantities (Booth, 2000; Fay et al., 2011; Punt, 2019a; see Online Supplementary Material for a discussion of the definition of "spatial structure"). Accounting for spatial structure can provide a greater degree of biological realism by 1) allowing for spatial variation in demographic parameters, 2) reducing the variance of fixed effect parameter estimates, and 3) more accurately reflecting the spatial dynamics of the fishing fleet(s), which may differ from those of fish population dynamics (Punt, 2019a). Spatially-structured assessments can inform rules for setting catch limits that respond to local dynamics (Bosley et al., 2019; McGarvey et al., 2017). They also can evaluate other types of spatial control mechanisms for fisheries management such as spatial closures within management zones, protected areas, and Territorial Use Rights for Fishing reserves (e.g., Kapur and Franklin, 2016; McGilliard et al., 2015; Field et al., 2006).

Problems for sustainable management can arise from a mismatch between management regions, which are often political, and the spatial extent of demographic population units, or stocks[1]. A stock can be defined by both its demography and the spatial area it inhabits. For example, Atlantic bluefin tuna (*Thunnus thynnus*) are comprised of two demographically distinct stocks inhabiting different areas with connectivity between them (National Research Council, 1994). Ignoring spatial structure in the assessment and management processes for such species may lead to local depletion (Benson et al., 2015; Goethel and Berger, 2016). For example, Morse et al., (2020) found that applying single-area models separately to each of two connected stocks in a simulation framework (i.e., ignoring spatial mixing) resulted in biased estimates of recruitment and spawning biomass for both stocks. Similarly, Ying et al., (2011) found that assessing and managing three mixed stocks of small yellow croaker (*Larimichthys polyactis*) off the coast of China as independent populations led to a high probability of overexploitation. As a corollary, assessing yellow croaker as a single stock, with the assumption of global recruitment, led to a high probability of local depletion. This echoes the findings from the previously mentioned simulation studies, and suggests that assumptions regarding the timing and locality of density dependence (recruitment) can influence the degree to which an assessment model diverges from the spatially-structured reality (Cadrin et al., 2019).

However, limited research has been undertaken to identify sustainable harvest rates that account for spatial structure and dynamics in a manner that matches spatial assessment assumptions. Reference points, which can be used to determine whether a stock is above or below a desired threshold either in terms of biomass or the degree of exploitation (which is ideally below a limit), bridge the assessment-management interface and the associated models used to calculate them can be adapted to account for spatial dynamics.

A salient feature of the next generation of stock assessment **models** will be accommodation of spatial heterogeneity **in mathematical representations of** fished populations and the fleets that exploit them (spatially-structured assessments; Punt et al., 2020). **The process of**

[1] We use the term "stock" to refer to a demographically unique or independent sub-population.

performing a stock assessment can involve data collection, processing, model selection, and the input of managers. Here, we are concerned with the functionality of stock assessment modeling packages. This distinction means that assessment scientists are able to design and run stock assessment model configurations that include various assumptions regarding the spatial structure of recruitment; whether and how these configurations are incorporated into the management process for a given stock is a decision left to the fishery management system in question.

Reference points are the bridge between the population model-fitting exercise and management implementation for many fisheries management agencies, including sovereign governments and international Regional Fishery Management Organizations (RFMOs). Reference points are quantities (most of which are based on the assumption that the population is in equilibrium, i.e., time-invariant selectivity, growth and fishing mortality) derived from population dynamics models. Common biomass reference points include unfished biomass, B_0, and the biomass at which maximum sustainable yield (MSY) is attained (B_{MSY}). Fishing mortality reference points include the fishing mortality rate at which MSY is attained (F_{MSY}), and the fishing mortality rate that maximizes the average yield from each recruit for a given size at first capture (F_{max}). Spawning biomass per recruit, SPR, can also be used as the basis for reference points. Typical SPR-based reference points include $F_{x\%}$, the fishing mortality corresponding to a x% reduction in SPR from unfished conditions and SPR_{MSY} the ratio of SPR when the population is fished at F_{MSY} to the SPR of the unfished population (Caddy and Mahon, 1995; Mangel et al., 2013).

Several of the generic stock assessment packages used worldwide include features to specify spatial population structure, and compute reference points (Table 1). However, in most cases, equilibrium yield-based reference points are defined by the assumption of spatially-aggregated recruitment (Francis and McKenzie, 2015). Some stock assessment packages provide reference points separately for each modelled area. **For example, CASAL/Casal2 (Table 1, Bull et al. 2012, Doonan et al., 2016) can account for natal homing and connectivity between different areas; both can provide estimates of unfished biomass (B_0), while CASAL provides yield estimates (MSY, B_{MSY}). In both cases, biomass can be calculated separately for the specified areas (Francis and McKenzie, 2015, T. A'mar, *pers. comm*), or as population-wide totals which are then allocated by area-specific fractions.**

Previous work has outlined the assumptions and decisions considered in spatial assessments (Berger et al., 2017; Cadrin et al., 2020; Punt, 2019a), and highlighted the modeling challenges posed by populations with varying demographics – or multiple stocks – inhabiting a managed region (Cadrin et al., 2019; Punt et al., 2017). **A spatial management approach does not require spatially explicit assessment or simulation models. Spatially structured modeling frameworks, including models that incorporate space both implicitly and explicitly, can be used directly to estimate reference points in a spatially explicit manner. They may also be used as operating models in a management strategy evaluation framework to find reference points that are not spatially defined, but are robust to uncertainty in spatial population structure and/or dynamics (Fig. 1). Non-spatially structured models can only provide reference point estimates that apply to the whole population, but those reference points may still be used in spatial management though the implementation of protected areas or spatial closures, or through the allocation of allowable catch in a spatially explicit manner. Thus, there are many paths to spatial management and tools need not be explicitly spatial to be useful in a spatial context.**

Spatially-structured assessments need to provide estimates of the reference points specific to a region or the prevailing fisheries management paradigm. Current methods are unable to do so accurately for certain spatial scenarios, specifically local productivity dynamics, which presents a barrier when designing and implementing next-generation assessment software. **One software package which approaches this issue is PRO-2BOX (Porch, 2018), which calculates MSY by finding the F-vector that maximizes the combined long-term yield from the two recruitment sources, which is subtly different from the combined long-term yield of each stock. A chief limitation of that approach is that it does not allow fish to change their stock affiliation (and thus movement characteristics) upon migration to another area. In the present simulation study, we demonstrate how the assumption of changed affiliation requires the use of an iterative optimization, and the implications of such an assumption on equilibrium reference points.**

Calculation of F_{MSY} (and hence B_{MSY} and MSY) [2] involves (numerically) solving the equation:

$$\frac{\delta C(F)}{\delta F}|_{F=F_{MSY}} = 0 \quad (1)$$

where $C(F)$ is the equilibrium yield when fully-selected fishing mortality is F. Equation 1 can be solved by simulation, which involves running the model to equilibrium (e.g., Goethel and Berger, 2016). Although simulation can be used to compute MSY-based reference points, this is computationally intensive and not easily integrated into software that analytically computes the uncertainty associated with reference points. It can be shown (see Section 2.1) that the calculation of $C(F)$ is analytical when recruitment is a function of the total spawning biomass (over all areas) and the proportion of the total recruitment that recruits to each area is independent of fishing mortality (and hence independent of the spawning biomass in each area). This "global" density-dependence assumption is the most common way recruitment is represented in stock assessment models used for tactical management (Table 1). However, another plausible way to represent the recruitment process is to assume that the recruitment to an area is functionally related to the biomass in that area ("local recruitment") (Cadrin et al., 2019; Porch, 2018). The need for next-generation stock assessment methods to include "local" density dependence in recruitment was highlighted by Punt (2019b) and Punt et al. (2020). We anticipate that an approach that considers area-specific productivity will be more sensitive to depletion in any linked area, and enable the identification of local depletion, which is a known problem with models that assume global recruitment (Okamoto et al., 2018).

We show how MSY-based reference points can be calculated for populations that exhibit local density-dependent recruitment. **The intention is to mathematically reconcile changes in the biomass in one area caused by the exploitation of fish within that area and other area(s) and by movement of biomass.** It is important to understand whether there are inherent properties of local recruitment that would lead to different (from previous) values for system wide *MSY*. We therefore develop a set of scenarios to compare the values for reference points given "global" and "local" recruitment. Our goal is to illustrate the functionality and tradeoffs associated with different assumptions about recruitment density dependence in spatial models, as local recruitment is being considered for implementation in future versions of Stock Synthesis (R. Methot, NOAA Fisheries, pers. comm). Finally, we describe the limitations posed by

[2] The focus here is on F_{MSY}, MSY and B_{MSY} because the other reference points outlined above are byproducts of their calculation.

existing management systems (both in the US and internationally) (Privitera-Johnson and Punt, 2020), and provide examples of how spatial reference points are implemented in management.

2. Methods

In this section, we derive and describe the calculation of MSY (and related reference points) under the common assumption that density dependence is global, and then introduce the relevant changes to this calculation when that assumption is violated, i.e., when density dependence is instead local to each area. This analysis compares the conventional ("global") assumption for calculating reference points such as F_{MSY} and B_{MSY} with an assumption that allows for local recruitment. In both cases, equilibrium recruitment is solved for as part of an optimization routine. **We then develop a simulation model to compare MSY estimates using the global and local assumption.** We present a simple single-sex, age-structured model with fishing throughout the year and two spatial areas (areas 1 and 2) to illustrate how spatially-articulated reference points differ depending upon the recruitment assumption used (Sections 2.1 and 2.2). In Equations 2-10, we use the letters ω and B to represent two theoretical spatial areas, noting that these could be extended to include more than two areas. The stock-recruitment relationship has the Beverton-Holt form, and fish are exploited by two fleets, each targeting a single area (*sensu* Sampson and Scott, 2011). A survival equation links age classes. Referring to the terminology introduced above, the analysis is comprised of two stocks for the local density dependence case – though some demographic parameters may be identical among areas, density-dependence can operate globally or locally within each area, resulting in two demographic units. **Several sensitivity tests are presented for the two MSY approaches by introducing systematic changes into the simulation model, such as in the demographic parameters (stock-recruitment steepness, natural mortality, weight-at-age), movement and fishery selectivity. The performance metrics used to compare the results among the two assumptions include: area-specific F_{MSY}, total yield, total B_{MSY} and area-specific depletion, the ratio of the biomass obtained at F_{MSY} to the unfished biomass (B_{MSY}/B_0).**

2.1 MSY and its definition in age-structured models with global density-dependence in recruitment

For the case in which the population dynamics model is spatial and the stock-recruitment relationship operates globally[3], $C(F)$ is calculated as:

$$C(F) = R(F)\tilde{C}(F) \tag{2}$$

where $\tilde{C}(F)$ is system-wide yield-per-recruit as a function of F, and $R(F)$ is global equilibrium recruitment when fully-selected fishing mortality is F. These quantities are defined as:

$$\tilde{C}(F) = \sum_{\omega}\sum_{a} w_a \frac{S_a^{\omega} F^{\omega}}{Z_a^{\omega}} \widetilde{N}_a^{\omega} \left(1 - e^{-Z_a^{\omega}}\right) \tag{3a}$$

$$\widetilde{N}_a^A = \begin{cases} \chi^{\omega} R(F) & \text{if } a = 0 \\ \widetilde{N}_{a-1}^{\omega} e^{-Z_{a-1}^{\omega}} \left(1 - \sum_{A' \neq A} \phi_{a-1}^{\omega,\omega'}\right) + \sum_{A' \neq A} \phi_{a-1}^{\omega',\omega} \widetilde{N}_{a-1}^{\omega'} e^{-Z_{a-1}^{\omega'}} & \text{otherwise} \end{cases} \tag{3b}$$

$$Z_a^{\omega} = M + S_a^F F^{\omega} \tag{3c}$$

[3] A single-area model is a special case of this model.

$$R(F) = \frac{R_0(4h\tilde{S}(F) - (1-h)\,\tilde{S}(0))}{(5h-1)\tilde{S}(F)} \quad (3d)$$

$$\tilde{S}(F) = \sum_\omega \sum_a f_a \tilde{N}_a^\omega \quad (3e)$$

where $\tilde{N}_a^\omega$ is the numbers-per-recruit in area ω of age a, Z_a^ω is the total mortality on animals of age a in area ω, S_a^ω is selectivity of animals of age a in area ω, F^ω is the fully-selected fishing mortality enacted in area ω, w_a is the weight of an animal of age a, M is an age- and time-invariant rate of natural mortality, $\tilde{S}$ is the spawning biomass-per-recruit by area, $\phi_a^{\omega,\omega'}$ is the probability of animals of age a in area ω moving to area ω' (after mortality), χ^ω is the **time-invariant** proportion of global recruitment to area ω, f_a is the fecundity of animals of age a, h is steepness of the stock-recruitment relationship (the expected proportion of unfished recruitment at 20% of unfished spawning biomass), and R_0 is unfished recruitment. Equation 3d arises from the following reparameterization of the Beverton-Holt stock-recruitment relationship:

$$R(F) = \frac{4hR_0R(F)\tilde{S}(F)}{(1-h)R_0\tilde{S}(0) + (5h-1)R(F)\tilde{S}(F)} \quad (4)$$

Equations 3a-c can be generalized in several ways including 1) allowance for multiple fleets in each area, 2) weight-at-age that varies spatially, 3) different stock-recruitment relationships, 4) different time of movement vs mortality, etc. Nevertheless, all of these formulations lead to yield being an analytical function of fully-selected fishing mortality[4]. To find F_{MSY} and associated quantities given global density-dependence, the values of the elements of the vector F^ω are found that maximize the system-wide yield (sum of yields in each area, MSY, Eqn. 1). This requires specification of the putative proportion of total recruitment that recruits to each area (i.e., χ^ω for each area(), which always sum to 1, and Beverton-Holt steepness h.

2.2 MSY and its definition in age-structured models with local density-dependence in recruitment

The presence of local density-dependence (e.g., stock-recruitment curves that operate independently in each area) involves modifying Eqns 2, 3a and 3b to **explicitly track the area-specific yield which results from a single recruit in each spawning area. This adjustment enables the yield curve to be defined, and thus the responsiveness of the yield-per-recruit for an areas to the net effect of fishing mortality and movement within and outside of that area.**

$$C(F) = \sum_B R^B(F) \sum_\omega \tilde{C}^{B,\omega}(F) \quad (5)$$

$$\tilde{C}^{B,\omega}(F) = \sum_a w_a \frac{S_a^\omega F^\omega}{Z_a^\omega} \tilde{N}_a^{B,\omega} \left(1 - e^{-Z_a^\omega}\right) \quad (6)$$

$$\tilde{N}_a^{B,\omega} = \begin{cases} 1 & \text{if } a = 0 \text{ and } \omega = B \\ 0 & \text{if } a = 0 \text{ and } \omega \neq B \\ \tilde{N}_{a-1}^{B,\omega} e^{-Z_{a-1}^\omega} \left(1 - \sum_{\omega' \neq \omega} \phi_{a-1}^{B,\omega,\omega'}\right) + \sum_{\omega' \neq \omega} \phi_{a-1}^{B,\omega',\omega} \tilde{N}_{a-1}^{B,\omega'} e^{-Z_{a-1}^{\omega'}} & \text{otherwise} \end{cases} \quad (7)$$

where $\tilde{C}^{B,\omega}(F)$ is yield in area ω based on a single recruit to area B as a function of F, $R^B(F)$ is equilibrium recruitment to area B when fully-selected fishing mortality is F, $\tilde{N}_a^{B,\omega}$ is the numbers

[4] Solution of Equation 1 requires a numerical solution of a non-linear equation.

in area ω of age a that were produced by one recruit that settled (at age 0) in area B, $\phi_a^{B,\omega,\omega'}$ is the probability of animals that originally settled to area B and currently in area ω moving to area ω' at age a (after mortality). ω' is any area different from ω, thus this syntax enables the inclusion of migration among two or more areas; the simulation study presented here only considers two areas. Importantly, fish that migrate into a given area are assumed to be completely assimilated into the population they migrate into, which other models have attempted to approximate by tracking the fraction of global recruitment that remains in or leaves their natal area (e.g., PRO-2BOX, Porch, 2018). This simulation study does not explicitly consider the growth of individual fish through time, which would require the assignment of **specific growth patterns** to settled recruits; the identity of a fish's **growth pattern** would shift depending on the area in which the fish is at age a. Given the assumption of area-specific density dependence and a Beverton-Holt stock recruitment relationship, the stock-recruitment relationship for each area (here ω) is given by:

$$R^{\omega}(F) = \frac{4h^{\omega}\chi^{\omega}R_0\sum_B \tilde{S}^{B,\omega}(F)R^B(F)}{(1-h^{\omega})\sum_B \tilde{S}^{B,\omega}(0)\chi^B R_0 + (5h^{\omega}-1)\sum_B \tilde{S}^{B,\omega}(F)R^B(F)} \quad (8)$$

where χ^{ω} is the proportion of the total (global) recruitment (**which was set without loss of generality to 1)**, to area ω in an unfished state, and

$$\tilde{S}^{B,\omega}(F) = \sum_a f_a \tilde{N}_a^{B,\omega} \quad (9)$$

Equation 8 is non-linear in $R^B(F)$; which reflects the key difference between global and local recruitment. Equation 8 can be solved iteratively by reorganizing it as:

$$4h^{\omega}\chi^{\omega}R_0\sum_B \tilde{S}^{B,\omega}(F)R^B(F) =$$

$$\left[(1-h^{\omega})\sum_B \tilde{S}^{B,\omega}(0)\chi^B R_0 + (5h^{\omega}-1)\sum_B \tilde{S}^{B,\omega}(F)R^B(F)\right]R^{\omega}(F) = \Upsilon_F^{\omega} \quad (10)$$

which is solved for $\underline{R}(F)$ using the R (R Core Team, 2020) function *optim*().

The process for calculating F_{MSY} in the case of local recruitment involves specifying the weight-at-age (perhaps by area), selectivity-at-age by fleet, natural mortality, steepness by area, R_0 and χ^{ω}, and then:

1. Using Equations 5-6, calculate the spawning biomass-per-recruit by area given no fishing in either area (F= 0; i.e. $\tilde{S}^{B,\omega}(0)$).
2. Given a value for F, calculate spawning biomass- and yield-per-recruit by area (Equations 9 and 5) and hence find the values for recruitment by area that satisfy Equation 10. Equation 1 can then be applied to calculate **equilibrium** catch given that F.
3. Repeat step 2 with different values for F until equation 1 is optimized.

2.3 Scenarios & Performance Metrics

Base Model

The reference points will differ depending on how recruitment is modelled ("global" vs "local"), with the effect depending on assumptions about growth, movement, fishery selectivity, natural mortality, and stock-recruitment steepness. Values for MSY-related quantities are therefore computed for "global" and "local" recruitment for a range of scenarios (Table 2). The unfished

biomass is the same for all scenarios and the remaining assumptions are the same for the two recruitment assumptions (where possible).

In the base-case scenario, recruitment is divided evenly between areas; we conduct an exploration of sensitivity to the proportion of recruitment to area 1 from 0.5 to 0.9. The probability of moving from area 2 to area 1 is a piecewise linear function of age (0 at age 0 increasing to a pre-specified movement rate at age 9 and constant thereafter; Fig. 2A). The base-case scenario assumes that area 1 is a sink area. The model specifies weight-at-age for each area. Ages are modelled from 0 (recruits) to 100 yr[5]. Fish length is specified by the von Bertalanffy growth curve, with an asymptotic length of 50 cm, an annual growth rate of 0.15 yr^{-1} and an age at length zero of 1, though results are insensitive asymptotic length. Weight is an allometric function of length following $w_{age} = aL_{age}^{b}$, where $a = 0.63$ and $b = 1.81$; we conduct a sensitivity to area-specific weights-at-age by increasing the age at length zero in area 1. Selectivity is an increasing logistic function of age, specified by ages at 50%- and 95%-selectivity, and can vary among areas. Fecundity-at-age is proportional to weight-at-age, with the ages at 50%- and 95%-maturity specified by area (although they are **the same in our simulations)**. The probability of moving is zero for age-0 fish, increases linearly to a maximum at age 9, after which all ages have the same movement rate. These movement rates vary between areas and among scenarios. **Fishing is assumed to occur on an annual basis before movement.**

The simplicity of this example is to illustrate the differences between the global and local density dependence. Therefore, the resulting differences in reference points can be attributed to the assumption about density-dependence and its interaction with the spatial transience created by movement between and differential exploitation among areas. **Code to reproduce the analyses from this manuscript can be found at** www.github.com/mkapur/sptlRP.

Alternative Scenarios (Sensitivity Runs)

Sensitivity is explored to no movement (the areas are completely independent, Fig. 2B), to varying degrees of exchange among areas (Figs. 2C-2E), to symmetric movement (Fig. 2F) and to several source-sink configurations (Figs. 2G-2J). Most of the scenarios are based on M=0.15yr^{-1} but sensitivity is explored to M=0.13yr^{-1} and M=0.17yr^{-1} ("low M" and "high M", respectively). Weight-at-age is the same in both areas for the base-case scenario (Fig. 2K), with sensitivity explored to higher weight-at-age in area 1 (Fig. 3A, "No movement, Higher WAA in area 2"). Selectivity is the same in the two areas for the base-case scenario (ages-at-50% and -95% selectivity of 9 and 13 years; Fig. 2L), with sensitivity explored to two alternative selectivity patterns (Figs 3B and 3C; "lower/higher age-at-50% selectivity in A1"). Stock-recruitment steepness is assumed to be 0.7 for both areas (0.7 for entire population for global density-dependence), with sensitivity explored to different (area-independent) values for steepness (0.6 and 0.8, "low/high h") as well to area-specific combinations thereof. **While not exhaustive, we selected these sensitivities to illustrate how commonly modeled processes with predictable impacts on single-area reference points influence equilibrium quantities when recruitment is assumed to be local.**

Performance metrics

Analyses are conducted for a base-case scenario and a range of sensitivity scenarios. Each scenario involved computing the two-dimensional yield curve surface with x- and y-axes defined by the fishing mortality by area and identifying the combination of area-specific fishing

[5] A sufficiently large number of years that the numbers at age 101+ are negligible even in an unfished state.

mortalities at which total yield is maximized (i.e., F_{MSY}). The results are articulated as system-wide totals, which is in keeping with many management systems, in which a single reference point will be calculated from a model comprised of more than one linked area.

4. Results

Each scenario (row) in Tables 2 and 3 took under one minute to optimize on a standard laptop computer, with the maximum iterations set to 1,000 and the vector of step sizes for the finite-difference approximation set to 1e-4 (the default is 1e-3). A finer step size is recommended as coarser (i.e., greater than 1e-2) search grids may cause the optimizer to overlook intermediate combinations of F_{MSY}. We specified the starting values for the two parameters at 0.47 after visualizing the yield surface (e.g., Fig. 4). The initial parameter estimate returned by optim() was then fed back into the same optimizer until the estimates did not change, for a maximum of five iterations. Scenarios with the base case movement parameterization required less than 100 function calls to find the local minimum, and fewer than 50 for the global case.

3.1 Base-case scenario

Fig. 4 shows the numbers-per-recruit in each region for the base-case scenario that includes area 1 as a sink. The numbers-per-recruit-at-age when summed over source area are identical between recruitment assumptions. The numbers-per-recruit in the area in which the animals did not settle is initially zero (as settlement is to a single area by construction) and increases given movement but declines to zero under mortality. The third row of Fig. 5 shows total yield as a function of fishing mortality by area for the case of global and local recruitment for the base-case scenario. The local recruitment assumption leads to a total MSY that is 15% higher than the global assumption, with a much higher F_{MSY} in the sink area, from which there is no movement of individuals back into the source area (Table 2).

3.2 Sensitivity analyses

The values for the reference points **and area-specific depletion at F_{MSY} (B_{MSY}/B_0)** are independent of movement rate if the two areas are identical (e.g., selectivity, weight-at-age and steepness h are the same) and movement is symmetric (Figs 4A-D, Table 3). This is true regardless of the proportion of recruitment that goes to each area (Table 3) because the local assumption estimates χ to be the same as the input proportion. Reference points scale up or down yet remain identical between assumptions if steepness or natural mortality increase or decrease by the same amount in each area (cases "No movement, low h", "No movement, high h", "No movement, low M", "No movement, high M"). However, the values of the reference points differ spatially when the areas differ in selectivity- or weight-at-age, or steepness. Higher weight-at-age in one area results in a higher F_{MSY} for that area if there is no movement between areas (case "No movement; Higher WAA in area 2"). Reducing the ages at 50%- and 95%-selectivity in one area also induces differences in F_{MSY} spatially, with a lower F_{MSY} in the area where fish are exploited at a younger age (case "No movement, low area 1 age-at-selectivity). The values for the reference points for combinations of steepness values among unlinked areas are identical to the values obtained for any scenario using that area-specific steepness value, e.g., a scenario with steepness of 0.6 in area 1 and 0.8 in area 2 produces the same reference point for area 1 as a scenario with a steepness of 0.6 in both areas in the absence of movement (cases "No movement, Combo h I" and "No movement, Combo h II").

3.3 Comparison of MSY-based reference points and depletion between local and global assumptions

Any degree of exchange (movement) among areas results in differences in reference points both among assumptions and between areas, with the local assumption consistently leading to a higher total MSY, with a lower corresponding total B_{MSY}, than the global assumption. In our simulation, out-migration from one area at levels of 30% or greater result in the global and local assumptions (cases "Area 2 as Sink I" and "Area 2 as Sink II") to estimate F_{MSY} at zero for the source area. The local assumption is less sensitive to increased movement, such that F_{MSY} remained zero in the source area when out-migration was 30% or 40% for ages 9 and older (cases "Exchange among Areas I" and "Exchange among Areas II"), whereas the global assumption estimated F_{MSY} in the source area to be $0.13yr^{-1}$ at 40% unidirectional movement (case "Exchange among Areas II"). Under a true source-sink dynamic ("Base Case" and cases "Area 2 as Sink I-IV"), the local assumption again leads to higher values of F_{MSY} for the sink area than the global assumption.

Reference points are the same between density-dependence assumptions when movement rates are the same between areas 1 and 2 and 2 and 1 (cases "No movement" and case "Symmetrical Movement"). The local assumption generally estimates F_{MSY} to be higher in the sink area than the source area and higher than the F_{MSY} defined for the sink area under the global assumption (cases "Area 2 as Sink I-IV"). The base-case scenario, which is characterized by a true source-sink dynamic (with area 1 as the sink), exhibits this same response (Table 3; Fig 3E-F). Reducing the age at which fish in area 1 are selected by the fishery in the base-case assumptions results in a decrease in F_{MSY} for area 1 and an increase in F_{MSY} for area 2 under both density-dependence assumptions, though this effect is much more pronounced for the global assumption (case "Base Case + low area 1 age-at-selectivity"). This is an expected outcome given the different assumptions' notions of equilibrium recruitment across the system.

MSY-based reference points for the local assumption are sensitive to area-specific exploitation and are generally less exploitative than the global approach of an area that is more vulnerable due to movement or demographics. In general, scenarios that include true source-sink dynamics and/or variation in steepness lead to the largest differences in reference points between the two density-dependence assumptions. **In such scenarios, depletion corresponding to MSY was uniformly higher (less depleted) in the sink area, which was the same result found in Goethel and Berger (2017). The local assumption also resulted in lower depletion levels corresponding to MSY than the global assumption for both areas.** The largest difference was found for a source-sink scenario with 40% of area 1 adults migrating to area 2, for which the global assumption produced a B_{MSY} that was 88% higher and MSY that was 20% lower than the local assumption (case "Area 2 as Sink I"). In a source-sink scenario with low movement from area 1 to area 2 (10%) these quantities were 18% greater and 8% lower, respectively (case "A2 as Sink IV"). B_{MSY} for scenarios with movement rates of 0.6 or higher did not vary more than 9% between density-dependence assumptions, while the corresponding MSY was only at most 2% higher for the local assumption (case "Exchange among Areas I-III"). When steepness varies among areas, the local assumption estimates area-specific F_{MSY} values that scale inversely with area-specific steepness, whereas F_{MSY} from the global assumption (which uses mean steepness) is equivalent.

Under a "pessimistic" version of the base-case scenario, where survivorship is low (high natural mortality) and steepness is reduced (case "Base Case + low h high M"), both density-dependence assumptions suggest an F_{MSY} of zero for the source area (area 2), while the F_{MSY} for

409 the sink area is nearly double for the local assumption ($0.6yr^{-1}$ vs $0.28yr^{-1}$). Conversely, under an
410 "optimistic" version of the base-case scenario (low *M* and increased steepness; case "Base Case
411 + high *h* low *M*") both density-dependence assumptions result in higher F_{MSY} for each area,
412 though the total MSY of the global assumption is 90% of the local assumption.
413 The results in Table 4, which are subject to some numerical variation, seem to suggest that
414 total F_{MSY} under the local assumption is conserved across scenarios with movement among
415 areas. This can be illustrated more clearly by allowing movement to mimic selectivity (so
416 movement within a source area appears like an additional fishery):
417

418
$$N_{a+1}^1 = N_a^1 e^{-M} e^{-S_a^1 F_1} e^{-S_a^1 Q}$$
$$N_{a+1}^2 = N_a^2 e^{-M} e^{-S_a^2 F_2} + N_a^1 e^{-M} e^{-S_a^1 F_1}(1 - e^{-S_a^1 Q}) \quad (11)$$

419
420 where *Q* is related to the proportion of individuals leaving area 1 for area 2 (area 2 is assumed to
421 be a sink area). In this formulation, fishing occurs before movement. Table 4 shows that in a
422 source-sink situation, with movement specified as in Equation 11, the total value of F_{MSY}
423 estimated using the local recruitment assumption is conserved across values of *Q* ranging from
424 0.1 to 0.9 (to the numerical accuracy of a discrete model). As in the main simulation results, the
425 greater proportion of fishing mortality is directed towards the sink area, and there is a movement
426 threshold (here about 40% transfer from area 1 to area 2) after which F_{MSY} in the source area is
427 reduced to zero. This result validates the rule of thumb (A.E. Punt, pers. comm.) that movement
428 can substitute for increased fishing mortality such that the F_{MSY} for a sink area is roughly twice
429 that expected for the entire population when two populations are of the same size in the absence
430 of fishing and the age-specific rates of movement have the same pattern as that of fishery
431 selectivity.

432 **4. Discussion**
433 *4.1 Spatial stock assessment and fisheries management*
434 Although the focus of this paper is on spatial stock assessments and hence the provision of
435 spatially-appropriate management advice, there are ways to produce the scientific advice that
436 may be needed to meet management mandates even when it is not possible to correctly represent
437 spatial structure (Fig. 1). These methods include allocating catch limits among fished areas based
438 on the relative abundance within sub-areas, or limiting effort outright by implementing Marine
439 Protected Areas, marine reserves, or closed areas. For example, catch limits determined from
440 assessments that do not explicitly include spatial dynamics or estimate spatial reference points
441 may be allocated among sub-stocks, based on a regional indicator of biomass, as is done for
442 Alaskan sablefish (*Anoplopoma fimbria*) (e.g., Hanselman et al., 2019). Bosley et al. (2019)
443 demonstrated that allocating catch limits in this manner can best approximate *MSY* in the absence
444 of a spatial model. Similarly, jack mackerel (*Trachurus murphyi*) is an ecologically and
445 commercially important pelagic fish in the south Pacific Ocean found in three regions (Arcos et
446 al., 2001; SPRFMO, 2019). The stock assessment process considers two hypotheses regarding
447 stock structure (single or two separate stocks). Under the two-stock hypothesis, the assessment
448 model is spatially-implicit because the fisheries operate in different areas and no mixing of the
449 stocks is assumed to occur. Management advice is based on comparing the *MSY* values from the
450 single-stock model with the sum of *MSY* from each area in the two-stock model. The most
451 precautionary advice (i.e., the lowest of the two *MSY*) is adopted for use (SPRFMO, 2019).
452 Likewise, data from a spatial assessment might be aggregated to estimate a reference point for

the whole stock (for example, reference points for rockfish on the US West Coast are calculated by area, then aggregated to determine TACs; R. Methot, *pers. comm.*). Finally, spatial management occurs in the case of marine protected areas and spatial closures, even when reference points are not estimated considering spatial structure (Anderson et al., 2019).

Assessments that do not have a spatial dimension can be tested for robustness to spatial population structure using a management strategy evaluation (MSE) with a spatial operating model (e.g., Morse et al., 2020). Studies using MSE to test the performance of non-spatial management for spatially structured populations have shown that more precautionary harvest rules can reduce the risk of overfishing in cases where spatial information is unknown or incorrectly specified. For example, in the case of Pacific herring (*Clupea pallasii*) in British Columbia, which have spatially distinct spawning grounds, management strategies that minimize exploitation risk can reduce the risk of overfishing when TACs are allocated based on a spatially-aggregated model (Benson et al., 2015).

Nevertheless, it is often better to explicitly include spatial structure in assessments. This is evident for small pelagic species, which exhibit both spatial structure and regime shift-like behavior through time. For example, biomass estimates for spatially-structured forage fish populations such as Pacific herring are biased when the assessment assumes a coarser spatial scale than that of the metapopulation dynamics (Benson et al., 2015). Punt et al. (2018) found that accounting for spatial structure improves hindcast performance and short-term forecasting when there is post-recruitment dispersal among sub-stocks, but the positive impact of including spatial structure was weaker when there was time-varying natural mortality (M). The development of reference points for ecosystem-based fisheries management (EBFM) of the Atlantic menhaden (*Brevoortia tyrannus*), another forage fish, has encountered similar challenges (Buchheister et al., 2017). Like Pacific herring, the potential for spatial variation in predation rates and temporal shifts in survival and productivity become confounded when spatial dynamics and temporal variation are both important. These examples highlight the importance of accounting for spatiotemporal interactions in assessments.

4.2 Including multiple sources of recruitment density-dependence in assessments

Our findings illustrate scenarios that lead to distinct MSY-based reference points between recruitment density-dependence assumptions. These scenarios are characterized by movement dynamics that accumulate biomass in one area (source-sink dynamics, namely those with strong unidirectional movement), or those in which either one or both areas are vulnerable to local depletion due to lower steepness, higher natural mortality, or a combination thereof. Generally, the local recruitment assumption suggests a rightward shift of the yield curve, leading to higher MSYs at lower system wide B_{MSY} (Fig. 6). This finding is consistent with the observation that spatial variation in fishing intensity (for example, in MPAs) can produce a "yield premium" above what would be gleaned by fishing the entire system at a single rate (Ralston et al., 2008). **In the presence of movement, yield curves are generally shallower (particularly under the local assumption) than in the absence of movement (see extent of yellow areas in Fig. 4). A similar finding was suggested by Bosley et al. (2019), who suggested that a greater number of area-specific F combinations could return similar yield goals when movement occurred among populations. It is possible that various configurations of area-specific F could return yields close to MSY, which has implications for spatial apportionment of fishing effort in an applied management context.**

Greater survivorship (lower M) or the ability to capture younger fish from one area can reduce the difference in reference points between assumptions in certain movement scenarios. In

the first case, lower *M* means greater overall population productivity in both areas, which reduces the relative differences between assumptions caused by asymmetrical movement dynamics. In the second, the fishery capitalizes on the biomass subsidy from the area with higher age-at-50% capture. These examples represent cases where calculating reference points based on local recruitment may not greatly change management advice. However, given the difficulty to estimate *M* with high precision, and the possibility of time-varying fishery selectivity **or apportionment**, it would be prudent to model the density dependence as faithfully as possible. Moreover, it would be fruitful to explore true spawning migration, larval dispersal and/or natal homing patterns when conducting assessments as these are factors suspected to render populations vulnerable to local depletion (Kerr et al., 2017). Time-varying movement, or the misalignment of management boundaries with biological regimes, presents a large hurdle for the calculation of spatial reference points (Berger et al., 2020). Our present approaches assume that equilibrium quantities are derived for a given movement and demographic regime; further simulation work could illustrate the degree to which temporal variation could accentuate or diminish discrepancies between areas. **It is possible that equilibrium frameworks such as these will not adequately address such situations.**

Incorporating spatial reference points into fisheries management may fulfill some management requirements, such as those of the Magnuson-Stevens Act (MSA) in the United States and the objectives of RFMOs. For example, the MSA mandates taking account of ecosystem considerations in fisheries management, which could include the consideration of spatial processes (Miller et al., 2018). **It is possible that equilibrium methods as the basis for reference point calculation may become untenable as models become increasingly complex representations of space and time. For example, Reuchlin-Hugenholtz et al. (2015) suggest that simple metrics of spatial distribution are strongly correlated with spawning stock biomass, and could be used to predict rapid population declines in population of fish species in the Northwest Atlantic. Incorporation of such spatio-temporal indices, which do not require the assumption of equilibrium may meet the requirement to determine** stock status relative to reference points that account for stock structure (MSA National Standard 3). Similarly, management bodies that operate based on a precautionary approach to management must consider spatial structure to limit the risk of local depletion and maintain stocks at levels that sustain optimum yield.

4.3 Conclusion

Management goals may not be met if stock structure is mis-specified in some part of the assessment process, which is particularly likely if the stock-recruitment relationship is local but is assumed to be global. This study demonstrates how accounting for local density dependence within spatial assessment models can be included in next generation stock assessment packages by illustrating how assessments that include spatial components can be extended to provide MSY-based reference points for local as well as global recruitment density-dependence assumptions. Unfortunately, Stock Synthesis (as well as several other assessment software used for tactical management, Table 1) does not accommodate area-specific stock-recruitment curves, although spatial structure is considered in SS via the calculation of area-specific spawning biomass. Consequently, differences in expected productivity between areas, and the subsequent impact on yields, are not represented. Local recruitment is being considered for implementation in future versions of Stock Synthesis (R. Methot, NOAA Fisheries, *pers. comm.*) and the approaches of this paper provide the technical basis for the necessary further development.

5. Acknowledgements

MCS was supported by a fellowship from the James S. McDonnell Foundation (Grant # 220020561). All other authors besides RM were funded by the Cooperative Institute for Climate, Ocean, and Ecosystem Studies (CICOES) under NOAA Cooperative agreement No. NA15OAR4320063. This manuscript was greatly improved by the feedback of three anonymous reviewers, as well as discussions with Dr. Clay Porch (the author of VPA-PRO2BOX).

6. References

Anderson, C.M., Krigbaum, M.J., Arostegui, M.C., Feddern, M.L., Koehn, J.Z., Kuriyama, P.T., Morrisett, C., Allen Akselrud, C.I., Davis, M.J., Fiamengo, C., Fuller, A., Lee, Q., McElroy, K.N., Pons, M., Sanders, J., 2019. How commercial fishing effort is managed. Fish Fish. 20, 268–285. https://doi.org/10.1111/faf.12339

Arcos, J.M., Oro, D., Sol, D., 2001. Competition between the yellow-legged gull *Larus cachinnans* and Audouin's gull *Larus audouinii* associated with commercial fishing vessels: The influence of season and fishing fleet. Mar. Biol. 139, 807–816. https://doi.org/10.1007/s002270100651

Begley, J., Howell, D., 2004. An overview of Gadget, the globally applicable area-disaggregated general ecosystem toolbox. ICES C 1–15.

Benson, A.J., Cox, S.P., Cleary, J.S., 2015. Evaluating the conservation risks of aggregate harvest management in a spatially-structured herring fishery. Fish. Res. 167, 101–113. https://doi.org/10/gg4skd

Berger, A.M., Goethel, D.R., Lynch, P.D., Quinn, T., Mormede, S., McKenzie, J., Dunn, A., 2017. Space oddity: The mission for spatial integration. Can. J. Fish. Aquat. Sci. 74, 1698–1716. https://doi.org/10/gg4q5g

Berger, A.M., Deroba, J.J., Bosley, K.M., Goethel, D.R., Langseth, B.J., Schueller, A.M., Hanselman, D.H., 2020. Incoherent dimensionality in fisheries management: consequences of misaligned stock assessment and population boundaries. ICES J. Mar. Sci. 78, 155–171. https://doi.org/10.1093/icesjms/fsaa203

Beverton, R.J.H., Holt, S.J., 1957. On the Dynamics of Exploited Fish Populations, Fisheries Investigations Series 2: Sea Fisheries. https://doi.org/10.1007/BF00044132

Booth, A.J., 2000. Incorporating the spatial component of fisheries data into stock assessment models 858–865. https://doi.org/10.1006/jmsc.2000.0816

Bosley, K.M., Goethel, D.R., Berger, A.M., Deroba, J.J., Fenske, K.H., Hanselman, D.H., Langseth, B.J., Schueller, A.M., 2019. Overcoming challenges of harvest quota allocation in spatially structured populations. Fish. Res. 220, 105344. https://doi.org/10.1016/j.fishres.2019.105344

Buchheister, A., Miller, T.J., Houde, E.D., 2017. Evaluating ecosystem-based reference points for Atlantic menhaden. Mar. Coast. Fish. 9, 457–478. https://doi.org/10/gg4sj9

Bull, B., Francis, R.I.C.C., Dunn, A., McKenzie, A., Gilbert, D.J., Smith, M.H., Bian, R., Fu, D., 2012. CASAL (C++ algorithmic stock assessment laboratory): CASAL User Manual v2.30-2012/03/21. Wellington, New Zealand.

Caddy, J.F., Mahon, R., 1995. Reference points for fisheries management. FAO Fish. Tech, Pap. No 347. FAO, Rome. 83pp.

Cadrin, S.X., Goethel, D.R., Morse, M.R., Fay, G., Kerr, L.A., 2019. "So, where do you come from?" The impact of assumed spatial population structure on estimates of recruitment. Fish. Res. 217, 156–168. https://doi.org/10.1016/j.fishres.2018.11.030

Cadrin, S.X., Maunder, M.N., Punt, A.E., 2020. Spatial Structure: Theory, estimation and application in stock assessment models. Fish. Res. 229, 105608. https://doi.org/10/ggv8sb

Doonan, I., Large, K., Dunn, A., Rasmussen, S., Marsh, C., Mormede, S., 2016. Casal2: New Zealand's integrated population modelling tool. Fish. Res. 183, 498–505. https://doi.org/10.1016/j.fishres.2016.04.024

Fay, G., Punt, A.E., Smith, A.D.M., 2011. Impacts of spatial uncertainty on performance of age structure-based harvest strategies for blue eye trevalla (*Hyperoglyphe antarctica*). Fish. Res. 110, 391–407. https://doi.org/10.1016/j.fishres.2011.04.015

Field, J.C., Punt, A.E., Methot, R.D., Thomson, C.J., 2006. Does MPA mean "Major Problem for Assessments"? Considering the consequences of place-based management systems. Fish Fish. 7, 284–302. https://doi.org/10.1111/j.1467-2979.2006.00226.x

Fournier, D.A., Hampton, J., Sibert, J.R., 1998. MULTIFAN-CL: A length-based, age-structured model for fisheries stock assessment, with application to South Pacific albacore, *Thunnus alalunga*. Can. J. Fish. Aquat. Sci. 55, 2105–2116. https://doi.org/10.1139/f98-100

Francis, R.I.C.C., McKenzie, J.R., 2015. Assessment of the SNA 1 stocks in 2013. New Zealand Fisheries

Assessment Report 2015/76. 82 pp.
Goethel, D.R., Berger, A.M., 2017. Accounting for spatial complexities in the calculation of biological reference points: Effects of misdiagnosing population structure for stock status indicators. Can. J. Fish. Aquat. Sci. 74, 1878–1894. https://doi.org/10.1139/cjfas-2016-0290
Hanselman, D.H., Rodgveller, C.J., Fenske, K.H., Shotwell, S.K., Echave, K.B., Malecha, P.W., Lunsford, C.R., 2019. Assessment of the sablefish stock in Alaska, Stock Assessment and Fishery Evaluation Report for the Groundfish Resources of the Gulf of Alaska. 605 W 4th Avenue, Suite 306, Anchorage, AK 99510. https://apps-afsc.fisheries.noaa.gov/refm/docs/2019/sablefish.pdf
Kapur, M.R., Franklin, E.C., 2017. Simulating future climate impacts on tropical fisheries: Are contemporary spatial fishery management strategies sufficient? Can. J. Fish. Aquat. Sci. 74, 1974–1989. https://doi.org/10.1139/cjfas-2016-0200
Kerr, L.A., Hintzen, N.T., Cadrin, S.X., Clausen, L.W., Dickey-Collas, M., Goethel, D.R., Hatfield, E.M.C., Kritzer, J.P., Nash, R.D.M., 2017. Lessons learned from practical approaches to reconcile mismatches between biological population structure and stock units of marine fish. ICES J. Mar. Sci. 74, 1708–1722. https://doi.org/10.1093/icesjms/fsw188
Mangel, M., MacCall, A.D., Brodziak, J., Dick, E.J., Forrest, R.E., Pourzand, R., Ralston, S., 2013. A perspective on steepness, reference points, and stock assessment. Can. J. Fish. Aquat. Sci. https://doi.org/10.1139/cjfas-2012-0372
McGarvey, R., Linnane, A., Matthews, J.M., Jones, A., 2017. Decision rules for quota setting to support spatial management in a lobster (*Jasus edwardsii*) fishery. ICES J. Mar. Sci. 74, 588–597. https://doi.org/10/gg5wxn
McGilliard, C.R., Punt, A.E., Methot, R.D., Hilborn, R., 2015. Accounting for marine reserves using spatial stock assessments. Can. J. Fish. Aquat. Sci. 72, 262–280. https://doi.org/10/gg5wxm
Methot, R.D., Wetzel, C.R., 2013. Stock synthesis: A biological and statistical framework for fish stock assessment and fishery management. Fish. Res. 142, 86–99. https://doi.org/10.1016/j.fishres.2012.10.012
Miller, Thomas J., et al. "Scientific Considerations Informing Magnuson–Stevens Fishery Conservation and Management Act Reauthorization: AFS Special Committee." *Fisheries* 43.11 (2018): 533-541.
Morse, M.R., Kerr, L.A., Galuardi, B., Cadrin, S.X., 2020. Performance of stock assessments for mixed-population fisheries: the illustrative case of Atlantic bluefin tuna. ICES J. Mar. Sci. https://doi.org/10/gg44r8
National Research Council (NRC), 1994. An Assessment of Atlantic Bluefin Tuna., The National Academies Press. Washington, DC. https://doi.org/https://doi.org/10.17226/4801
Okamoto, D.K., Hessing-Lewis, M., Samhouri, J.F., Shelton, A.O., Stier, A., Levin, P.S., Salomon, A.K., 2020. Spatial variation in exploited metapopulations obscures risk of collapse. Ecol. Appl. 30, 1–16. https://doi.org/10.1002/eap.2051
Porch, C., 2018. PRO-2BOX 3.0 User Guide (No. NMFS-SEFSC-708). https://doi.org/10.13140/RG.2.2.12258.17604
Privitera-Johnson, K.M., Punt, A.E., 2020. A review of approaches to quantifying uncertainty in fisheries stock assessments. Fish. Res. 226, 105503. https://doi.org/10.1016/j.fishres.2020.105503
Punt, A.E., Haddon, M., Little, L.R., Tuck, G.N., 2017. The effect of marine closures on a feedback control management strategy used in a spatially aggregated stock assessment: a case study based on pink ling in Australia. Can. J. Fish. Aquat. Sci. 74, 1960–1973. https://doi.org/10.1139/cjfas-2016-0017
Punt, A.E., Okamoto, D.K., MacCall, A.D., Shelton, A.O., Armitage, D.R., Cleary, J.S., Davies, I.P., Dressel, S.C., Francis, T.B., Levin, P.S., Jones, R.R., Kitka, H., Lee, L.C., McIsaac, J.A., Poe, M.R., Reifenstuhl, S., Silver, J.J., Schmidt, J.O., Thornton, T.F., Voss, R., Woodruff, J., 2018. When are estimates of spawning stock biomass for small pelagic fishes improved by taking spatial structure into account? Fish. Res. 206, 65-78. https://doi.org/10.1016/j.fishres.2018.04.017
Punt, A.E., 2019a. Spatial stock assessment methods : A viewpoint on current issues and assumptions. Fish. Res. 213, 132–143. https://doi.org/10.1016/j.fishres.2019.01.014
Punt, A.E., 2019b. Modelling recruitment in a spatial context: A review of current approaches, simulation evaluation of options, and suggestions for best practices. Fish. Res. 217, 140–155. https://doi.org/10.1016/j.fishres.2017.08.021
Punt, A.E., Dunn, A., Elvarsson, B. Þór, Hampton, J., Hoyle, S.D., Maunder, M.N., Methot, R.D., Nielsen, A., 2020. Essential features of the next-generation integrated fisheries stock assessment package: A perspective. Fish. Res. 229, 105617. https://doi.org/10.1016/j.fishres.2020.105617
R Core Team, 2020. R: a language and environment for statistical computing. R Foundation for Statistical Computing, Vienna, Austria. URL https://www.R-project.org/

Ralston, S., O'Farrell, M. R., 2008. Spatial variation in fishing intensity and its effect on yield. Can. J. Fish. Aquat. Sci. 65, 588-599. https://doi.org/10.1139/f07-174

Reuchlin-Hugenholtz, E., Shackell, N.L., Hutchings, J.A., 2015. The potential for spatial distribution indices to signal thresholds in marine fish biomass. PLoS One 10, 1–22. https://doi.org/10.1371/journal.pone.0120500

Sampson, D.B., Scott, R.D., 2011. A spatial model for fishery age-selection at the population level. Can. J. Fish. Aquat. Sci. 68, 1077–1086. https://doi.org/10.1139/F2011-044

SPRFMO, 2019. 7th Scientific Committee meeting report. Wellington, New Zealand. 98 pp.

Schaefer, M.B., 1968. Methods of Estimating Effects of Fishing on Fish Populations. Trans. Am. Fish. Soc. 97, 231–241. https://doi.org/10.1577/1548-8659(1968)97[231:moeeof]2.0.co;2

Ying, Y., Chen, Y., Lin, L., Gao, T., 2011. Risks of ignoring fish population spatial structure in fisheries management. Can. J. Fish. Aquat. Sci. https://doi.org/10.1139/F2011-116

7. Tables

Table 1. Commonly used generic stock assessment frameworks that include spatial structure and the *F*-based reference points they estimate.

Model	Primary citation(s)	Spatial structure	Movement Dynamics	Other features (multispecies, ecosystem, etc.)	Reference points	Spatial reference points
Globally applicable Area-Disaggregated General Ecosystem Toolbox (GADGET)	Begley and Howell (2004)	Multiple areas linked by movement	Movement between stocks based on age and maturity status	Multi-species and multi-stock	F_{MAX}	None available
Multiple Length Frequency Analysis with Catch-at-Length (MULTIFAN-CL)	(Fournier et al., 1998)	Multiple areas linked by movement	Limited movement, diffusive	Multi-stock	F_{MSY}	Area level, groups of areas or the whole model domain
Stock Synthesis (SS)	(Methot and Wetzel, 2013)	Multiple areas linked by movement	Age-specific	Single-stock	F_{MAX}, F_{MSY}, $Fx\%$	Assume global recruitment
C++ Algorithmic Stock Assessment Laboratory (CASAL/Casal2)	Bull et al. (2012) & Doonan et al. (2016)	Multiple areas linked by movement	Movement dynamics allow natal homing	Multi-stock	*CASAL:* F_{MSY}, $Fx\%$ *Casal2:* B_0 **(no MSY-based reference points)**	Sum of B_0 across areas, **or allocate to areas using pre-defined fraction**
Dual Zone VPA Model (VPA-2BOX)	Porch (2018)	Two stocks	Users choose between two types of box-transfer models to simulate intermixing between the two stocks: diffusion and overlap	Two stocks	F_{MSY}, $Fx\%$	Stock specific; in overlap case recruits are tracked based upon spawning area

Table 2. Specifications for the scenarios. A dash indicates that the specification matches that of the base-case scenario.

Scenario	Proportion of recruitment to area 1	Natural mortality (yr^{-1})	Weight- at-Age	Movement	Selectivity	Steepness
Base case (Area 1 as sink)	0.5	0.15	Fig. 2K	Fig. 2A	Fig. 2L	0.7, 0.7
No movement $\chi^1 = 0.5$	-	-	-	Fig. 2B	-	-
No movement $\chi^1 = 0.6$	0.6	-	-	Fig. 2B	-	-
No movement $\chi^1 = 0.7$	0.7	-	-	Fig. 2B	-	-
No movement $\chi^1 = 0.8$	0.8	-	-	Fig. 2B	-	-
No movement $\chi^1 = 0.9$	0.9	-	-	Fig. 2B	-	-
No movement, Higher WAA in area 2	-	-	Fig. 3A	Fig. 2B	-	-
No movement, low area 1 age-at-selectivity	-	-	-	Fig. 2B	Fig. 3B	-
No movement, low *h*	-	-	-	Fig. 2B	-	0.6, 0.6
No movement, high *h*	-	-	-	Fig. 2B	-	0.8, 0.8
No movement, combo *h* I	-	-	-	Fig. 2B	-	0.6, 0.8
No movement, combo *h* II	-	-	-	Fig. 2B	-	0.8, 0.6
No movement, low *M*	-	0.13	-	Fig. 2B	-	-
No movement, high *M*	-	0.17	-	Fig. 2B	-	-
Exchange among Areas I	-	0.17	-	Fig. 2C	-	-
Exchange among Areas II	-	0.17	-	Fig. 2D	-	-
Exchange among Areas III	-	0.17	-	Fig. 2E	-	-
Symmetrical Movement	-	-	-	Fig. 2F	-	-
Area 2 as Sink I	-	-	-	Fig. 2G	-	-
Area 2 as Sink II	-	-	-	Fig. 2H	-	-
Area 2 as Sink III	-	-	-	Fig. 2I	-	-
Area 2 as Sink IV	-	-	-	Fig. 2J	-	-
Base Case + low area 1 age-at-selectivity	-	-	-	-	Fig. 3B	-
Base Case + high area 1 age-at-selectivity	-	-	-	-	Fig. 3C	-
Base Case + combo *h*	-	-	-	-	Fig. 2L	0.8, 0.6
Base Case + low *h* high *M*	-	0.17	-	-	Fig. 2L	0.6, 0.6
Base Case + high *h* low *M*	-	0.13	-	-	Fig. 2L	0.8, 0.8

Table 3. Results for the scenarios and values for reference points for each assumption. The values for F_{MSY} are the fully-selected fishing mortality rates by area, the MSY ratio is MSY for global recruitment relative to that for local recruitment, and B_{MSY}/B_0 is total spawning biomass at MSY relative to unfished spawning biomass. A dash indicates that the specification matches that of the base-case scenario.

Scenario	F_{MSY} (area 1, area 2) yr^{-1}		MSY	B_{MSY}/B_0 (area 1, area 2)	
	Global	Local	Ratio (global/local)	Global	Local
Base case (Area 1 as sink)	0.33, 0.03	0.57, 0.02	0.85	0.26, 0.26	0.26, 0.26
No movement $\chi^1 = 0.5$	0.27, 0.27	0.27, 0.27	1	0.26, 0.26	0.26, 0.26
No movement $\chi^1 = 0.6$	0.27, 0.27	0.27, 0.27	1	0.26, 0.26	0.27, 0.27
No movement $\chi^1 = 0.7$	0.27, 0.27	0.27, 0.27	1	0.26, 0.26	0.27, 0.26
No movement $\chi^1 = 0.8$	0.27, 0.27	0.27, 0.27	1	0.26, 0.26	0.26, 0.27
No movement $\chi^1 = 0.9$	0.27, 0.27	0.27, 0.27	1	0.33, 0.20	0.26, 0.27
No movement, Higher WAA in area 2	0.19, 0.36	0.25, 0.27	1	0.42, 0.13	0.30, 0.24
No movement, low area 1 age-at-selectivity	0.16, 0.48	0.23, 0.28	1.01	0.30, 0.30	0.30, 0.30
No movement, low *h*	0.20, 0.20	0.20, 0.20	1	0.22, 0.22	0.22, 0.22
No movement, high *h*	0.39, 0.39	0.39, 0.39	1	0.21, 0.3	0.32, 0.21
No movement, combo *h* I	0.27, 0.27	0.2, 0.39	1	0.3, 0.21	0.21, 0.32
No movement, combo *h* II	0.27, 0.27	0.39, 0.20	1	0.27, 0.27	0.27, 0.27
No movement, low *M*	0.23, 0.23	0.23, 0.23	1	0.26, 0.26	0.26, 0.26
No movement, high *M*	0.33, 0.33	0.33, 0.33	1	0.39, 0.14	0.37, 0.12
Exchange among Areas I	0.45, 0	0.50, 0	0.97	0.36, 0.17	0.32, 0.17
Exchange among Areas II	0.42, 0.13	0.59, 0	0.97	0.32, 0.21	0.28, 0.22
Exchange among Areas III	0.39, 0.24	0.55, 0.11	0.98	0.26, 0.26	0.26, 0.26
Symmetrical Movement	0.27, 0.27	0.27, 0.27	1	0.02, 0.53	0.02, 0.33
Area 2 as Sink I	0, 0.29	0, 0.59	0.8	0.05, 0.5	0.04, 0.33
Area 2 as Sink II	0, 0.30	0, 0.59	0.81	0.11, 0.44	0.10, 0.32
Area 2 as Sink III	0.03, 0.33	0.02, 0.57	0.85	0.18, 0.36	0.15, 0.32
Area 2 as Sink IV	0.17, 0.32	0.17, 0.43	0.92	0.44, 0.11	0.32, 0.10
Base Case + low area 1 age-at-selectivity	0.23, 0.28	0.42, 0.04	0.86	0.51, 0.06	0.38, 0.08
Base Case + high area 1 age-at-selectivity	0.42, 0	0.78, 0.01	0.84	0.39, 0.15	0.27, 0.12
Base Case + combo *h*	0.33, 0.03	0.73, 0	0.78	0.50, 0.11	0.28, 0.10
Base Case + low *h* high *M*	0.28, 0	0.60, 0	0.78	0.52, 0.13	0.33, 0.10
Base Case + high *h* low *M*	0.38, 0.07	0.55, 0.08	0.90	0.37, 0.09	0.30, 0.08

Table 4. Results for vignette scenarios, in which the age-specific pattern of movement matches selectivity (Equation 11). The proportion of recruitment to area 1, natural mortality, selectivity and stock-recruitment steepness are as for the base-case scenario (Table 2). Q^1 is the proportion of individuals of all ages which move out of area 1 for area 2, where they remain.

Scenario	Proportion movement out of area 1 and area 2	F_{MSY} (area 1, area 2) yr^{-1}		Total local F_{MSY} yr^{-1}	MSY ratio (global/local)	B_{MSY}/B_0	
		Global	Local			Global	Local
Vignette $Q^1 = 0.10$	0.1, 0	0.22, 0.32	0.3, 0.29	0.59	0.97	0.26	0.25
Vignette $Q^1 = 0.20$	0.2, 0	0.15, 0.37	0.28, 0.33	0.61	0.94	0.27	0.24
Vignette $Q^1 = 0.25$	0.25, 0	0.11, 0.39	0.28, 0.35	0.63	0.93	0.27	0.24
Vignette $Q^1 = 0.30$	0.3, 0	0.08, 0.42	0.26, 0.37	0.63	0.92	0.27	0.23
Vignette $Q^1 = 0.35$	0.25, 0	0.04, 0.45	0.24, 0.39	0.63	0.91	0.27	0.23
Vignette $Q^1 = 0.40$	0.4, 0	0, 0.47	0.22, 0.41	0.63	0.90	0.27	0.22
Vignette $Q^1 = 0.50$	0.5, 0	0, 0.43	0, 0.59	0.59	0.90	0.27	0.24
Vignette $Q^1 = 0.60$	0.6, 0	0, 0.4	0, 0.59	0.59	0.88	0.27	0.22
Vignette $Q^1 = 0.70$	0.7, 0	0, 0.38	0, 0.6	0.60	0.87	0.27	0.21
Vignette $Q^1 = 0.80$	0.8, 0	0, 0.37	0, 0.59	0.59	0.86	0.27	0.20
Vignette $Q^1 = 0.90$	0.9, 0	0, 0.36	0, 0.6	0.60	0.86	0.27	0.20
Vignette no movement	0, 0	0.27, 0.27	0.27, 0.27	0.54	1.00	0.26	0.27
Vignette symmetrical movement	0.3, 0.3	0.27, 0.27	0.27, 0.27	0.54	1.00	0.26	0.27

8. Figures

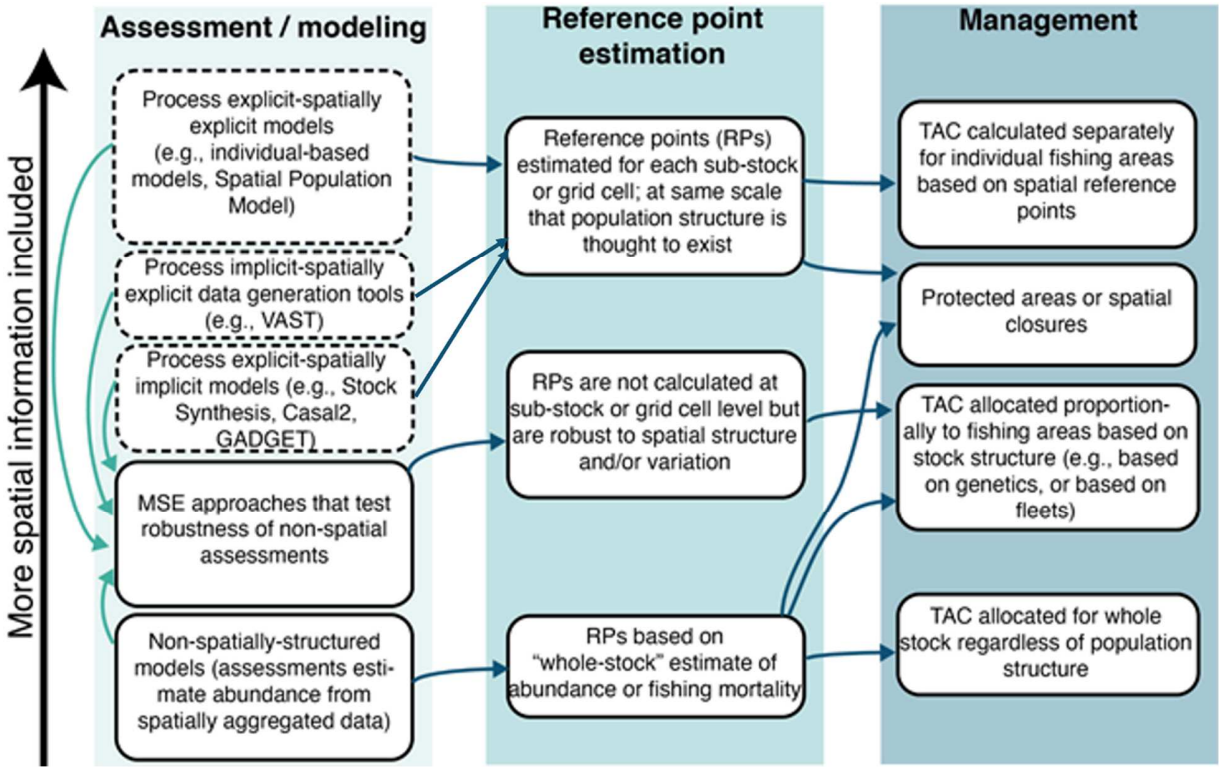

Figure 1. A schematic of how spatial information is used to estimate reference points for management and when implementing spatial management. Arrows indicate pathways through which information is used in science and management. Lighter arrows indicate where spatial models and data generation tools are used to improve management science, and dark arrows indicate ways that spatial information is or is not turned into spatial management practices. Spatially structured models and data-generation tools (dashed lines) consider differences in population dynamics among areas. See the Online Supplementary Material for a discussion of the distinction between process- and spatially-explicit vs. implicit models.

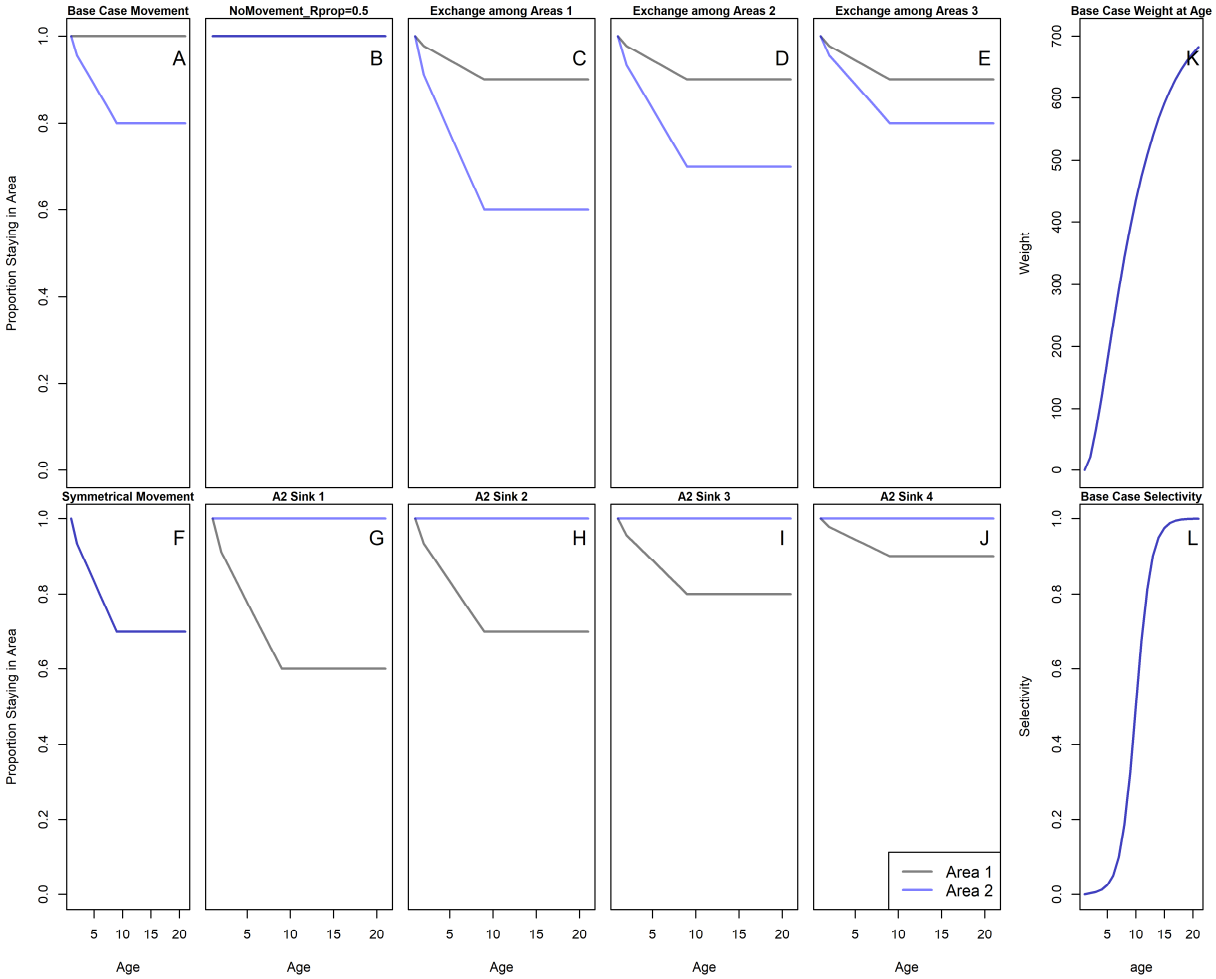

Figure 2. Age-specific specifications for the scenarios. A-J) Movement at age. Values indicate the proportion of individuals that remain in each area (colors) at each age. K) Weight-at-age for the base-case scenario, which is identical between areas. E-G) Fishery selectivity-at age for the base-case scenario, which is identical between areas. All values are identical for ages 20+.

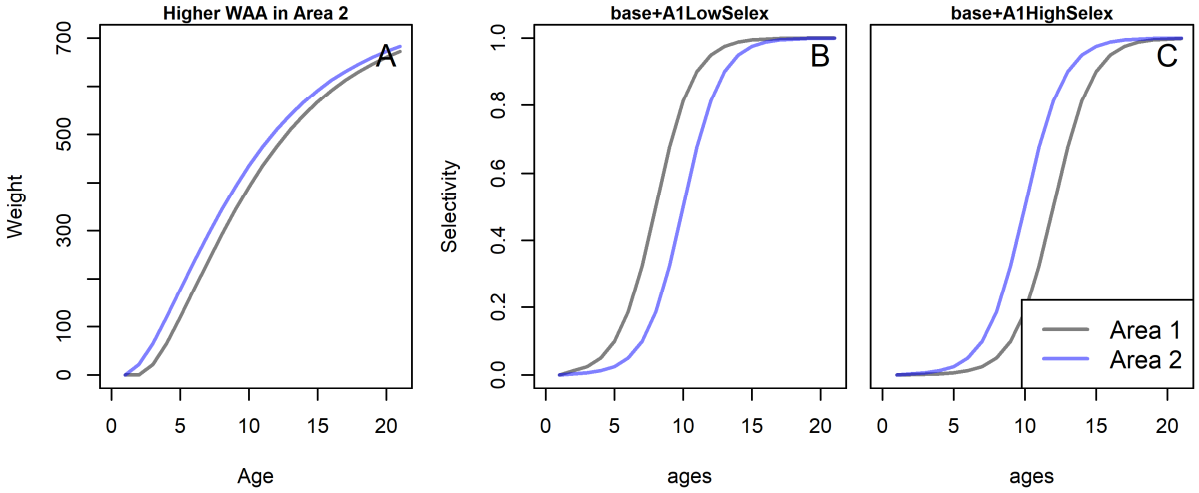

Figure 3. A) Weight-at-age for the "Higher Weight at Age in area 2" scenario. B) Fishery selectivity-at-age by area for scenarios that include lower selectivity at age in area 1. C) Fishery selectivity-at-age by area for scenarios that include higher selectivity at age in area 1. All values are identical for ages 20+.

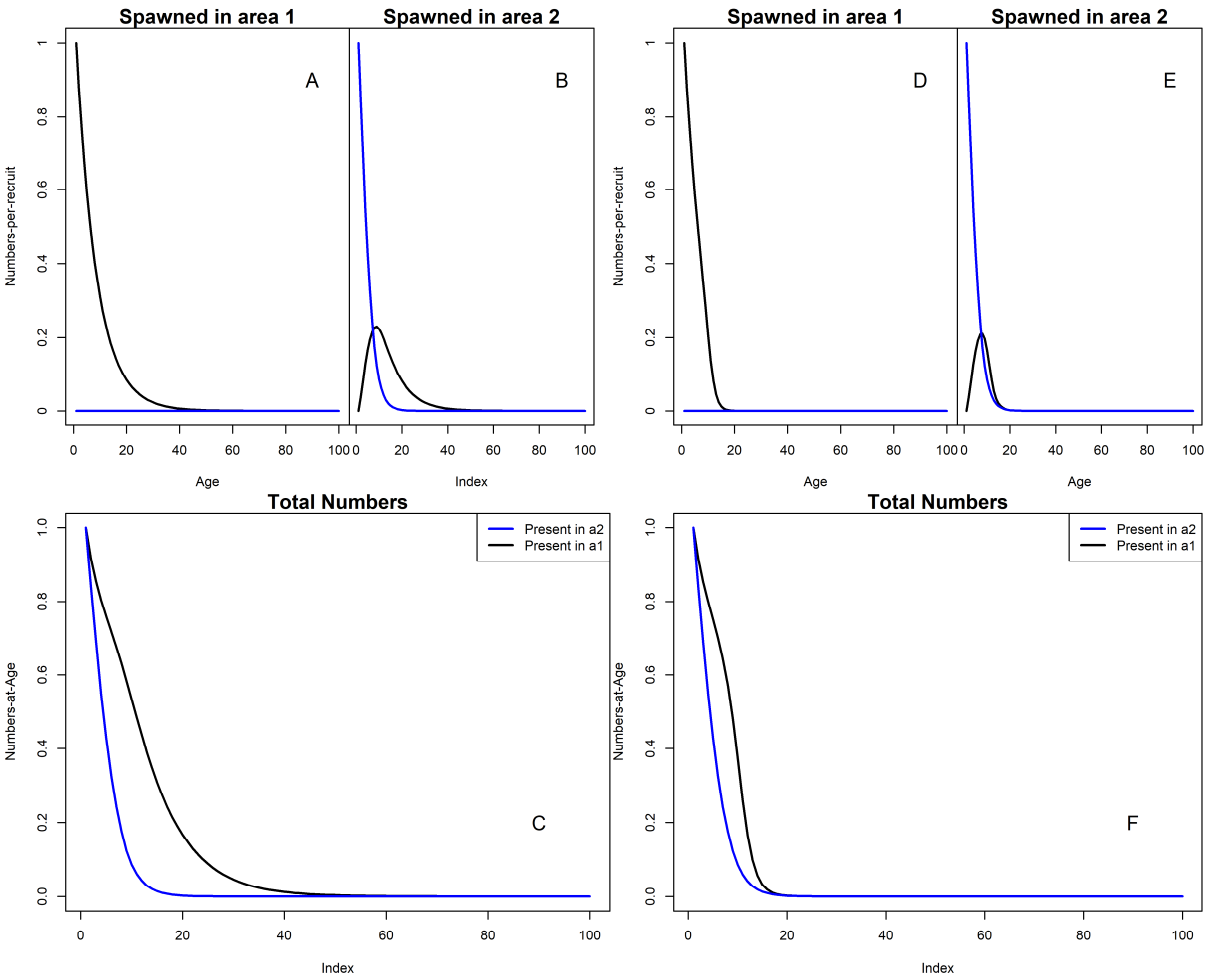

Figure 4. Equilibrium numbers-per-recruit (top row) and -at-age (bottom row) based on spawning origin for the base-case scenario (area 1 as sink) under F=0 (A-C) and F=F_{MSY} (D-F). Figures A and D indicate the fate in numbers-at-age of a single recruit spawned in area 1; Figures B and E indicates the same for a recruit spawned in area 2; Figures C and F indicate the total numbers-per-recruit in each area under two different values for F. In each plot, blue lines represent individuals found in area 2 and black lines indicate those found in area 1.

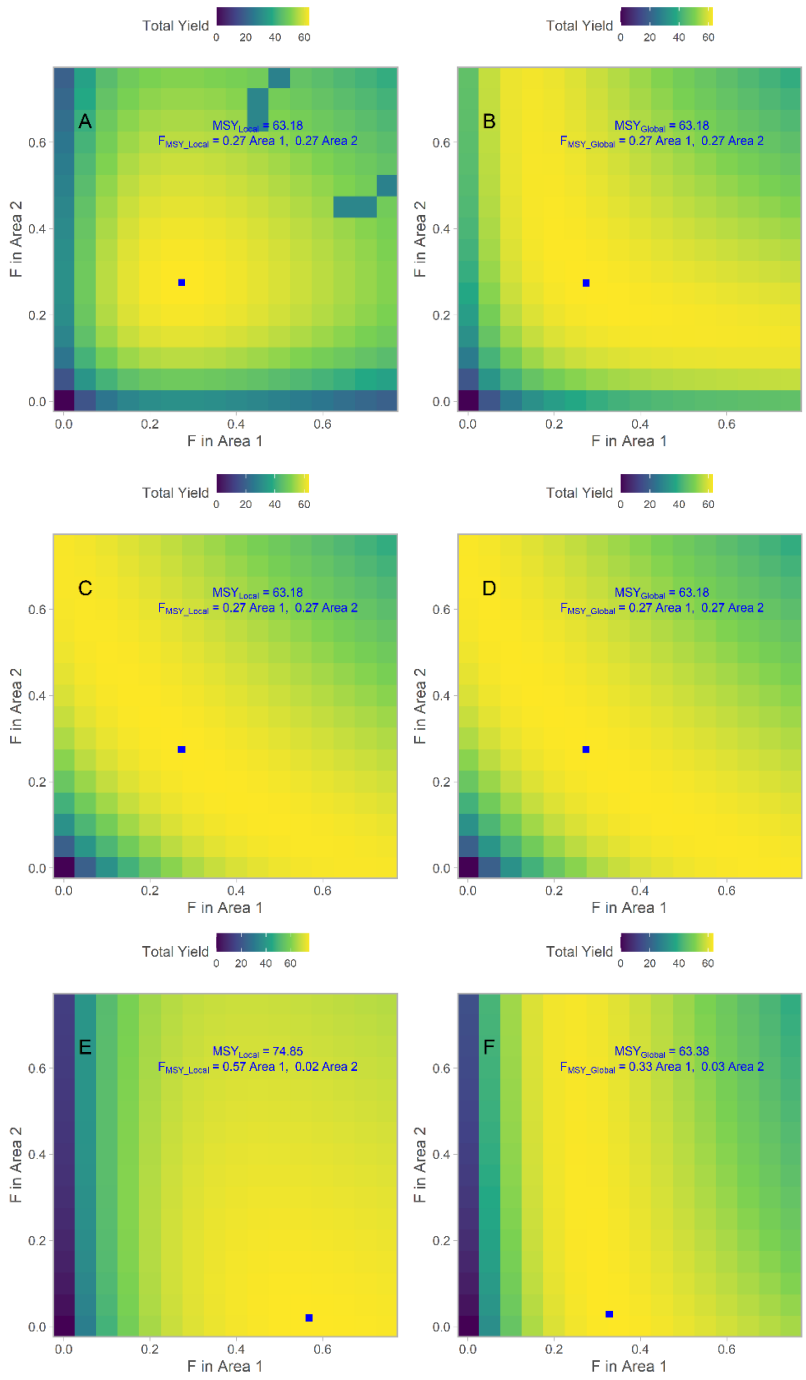

Figure 5. Total yield as a function of fishing mortality (yr^{-1}) by area for the local and global assumptions (left and right columns) for three scenarios: A-B) the first no-movement case, with χ^1 set to 0.5; C-D) a movement with symmetric exchange among areas, and E-F) the base-case scenario. The colors denote total yield and the solid square point indicates F_{MSY}.

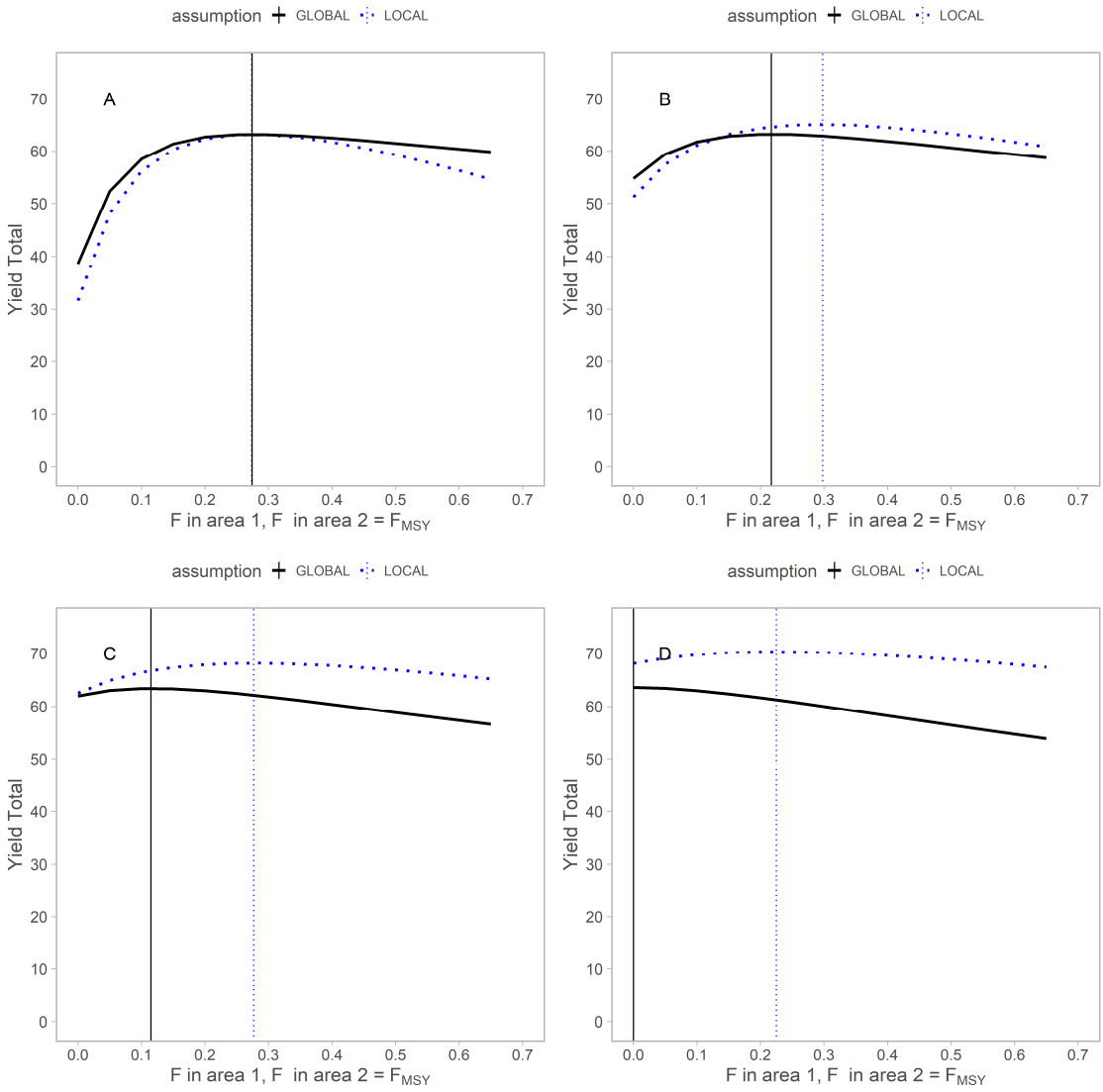

Figure 6. Illustration of the rightward shift of the yield curve due local density dependence for four scenarios (Table 2): A) No movement, input $\chi = 0.5$, B) C) D). In all figures, the x-axis represents various values of F (yr^{-1}) for area 1. Yield curves are generated by fixing F in area 2 to F_{MSY} for area 2 for the scenario in question. The vertical lines indicate the location of F_{MSY} in area 1. Blue dotted lines = local recruitment assumption, black solid lines = global recruitment assumption.